Proceedings of the 5th WSEAS International Conference on Telecommunications and Informatics, Istanbul, Turkey, May 27-29, 2006 (pp226-231)

Computation of Characteristic Impedance of CPW, Grounded CPW (GCPW) and Microstrip Lines in a Wide Frequency Range Using TLM Approach

H. KEIVANI M. FAZAELIFARD M. FARROKHROOZ
Islamic Azad University, Branch of Kazeroun,
Kazeroun, Iran

Abstract: Transmission lines analysis in high frequencies needs use of full wave numerical approaches like TLM (Transmission Line Matrix) which is one of the powerful and useful approaches in electromagnetism. It can be used for analysis of structures of geometrical or non-geometrical forms, isotropic, non-isotropic, homogenous or non-homogenous structures and other structures with or without of electrical or magnetic losses. In this paper we use TLM approach to compute the characteristic impedance of microstrips and transmission lines like Planar Waveguide (CPW) and Grounded Planar Waveguide (GCPW).In previous works, ε_{effect} has been used for computing characteristic impedance of transmission lines in high frequencies (several GHz) [1] but calculation of ε_{effect} without using full wave numerical methods is not accurate enough. The lack of accuracy is caused by effect of fringing, effects of thickness, effects of scattering and semi-static conditions. In this paper, we will review TLM network exciting, computation of fields, selecting method for mesh dimensions and timestep. Finally we will present the computation results of characteristic impedance for mentioned structures.

Keywords: Characteristic Impedance Z_{ol} , TLM, CPW, GCPW, and GSCN

1- Introduction

2D-TLM and 3D-TLM are the main TLM numerical approaches. 2D-TLM consist of two categories: 2D-TLM with series nodes and 2D-TLM with parallel nodes [2].
The propagation of TE mode waves is studied using series nodes and parallel nodes are used for TM mode waves studying.
Each of these categories can model three components of electromagnetic fields. Modeling of all six components of electromagnetic fields will be possible using 3D-TLM.

A. 3D-TLM with expanded node:

H_z, H_x, E_y can be modeled using composition of two series and one parallel nodes and a composition of two series and one parallel nodes can model E_z,H_y,E_x [2,3].
There is a $\Delta l/2$ distance between each of the series nodes (magnetic fields) and parallel
Nodes (electric fields), therefore this structure is called Expended Node TLM.
There are some disadvantages for this approach [4]:

1- Complexity in Expanded Node structure.
2-The electric and magnetic fields are calculated separately with a $\Delta l/2$ distance.
3- Difficulty in using boundary conditions.

B. Condensed Node 3D-TLM

To cope with above difficulties, P. B. Johns presented the Symmetrical Condensed Node (SCN) [5]. Fig.1 shows a Symmetrical Condensed Node.
There are some advantages for SCN:
1- All six components of fields can be computed simultaneously.
2- Because of symmetry, the boundaries, loss materials and non-homogenous structures can be modeled easily.
The SCN has various types; HSCN, SSCN, ASCN, and GSCN. We will begin the explanation of these types of SCN by introducing GSCN (General SCN),

because its formulation is in general form and it can be used for all types of SCN.

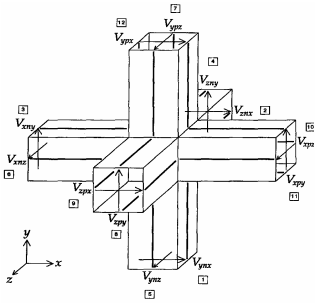

Fig.1: A Symmetrical Condensed Node.

2- The Computation Of Electromagnetic Fields

2-1 Computation of electrical fields

Fig.2 is a part of SCN shown in Fig.1 that is in the direction of Z-axis. The matched stub (V_{ez}) and open circuit stub (V_{oz}) have been added to SCN node for modeling of electrical losses and permittivity (ε), respectively.
In Fig.2 we have [6]:

$$V_z = \frac{2(V^i_{xnz}y_{xnz} + V^i_{xpz}y_{xpz} + y_{ynz}V^i_{ynz} + y_{ypz}V^i_{ypz} + y_{0z}V^i_{0z})}{y_{xnz} + y_{xpz} + y_{ynz} + y_{ypz} + y_{0z} + G_z} \quad (1)$$

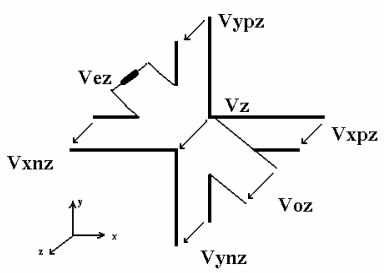

Fig2. GSCN node with open and matched circuit stubs

Using Equ.1, we can achieve to two similar equations for V_x and V_y as below:

$$V_x = \frac{2(V^i_{ynx}y_{ynx} + V^i_{ypx}y_{ypx} + y_{znx}V^i_{znx} + y_{zpx}V^i_{zpx} + y_{0x}V^i_{0x})}{y_{ynx} + y_{ypx} + y_{znx} + y_{zpx} + y_{0x} + G_x} \quad (2)$$

$$V_y = \frac{2(V^i_{xny}y_{xny} + V^i_{xpy}y_{xpy} + y_{zny}V^i_{zny} + y_{zpy}V^i_{zpy} + y_{0y}V^i_{0y})}{y_{xny} + y_{xpy} + y_{zny} + y_{zpy} + y_{0y} + G_y} \quad (3)$$

Where y_{inj} and y_{ipj} are characteristic admittance of transmission lines, y_{oi} is admittance of open circuit stub and G_i is the conductance of matched stub $(i, j \in x, y, z)$ Above values can be calculated as explained in [7].
Using Equs.1-3, we can compute electrical fields in a TLM mesh of $\Delta x \times \Delta y \times \Delta z$ dimension.

$$E_x = -V_x/\Delta x, E_y = -V_y/\Delta y, E_z = -V_z/\Delta z \quad (4)$$

2-2 Computation of magnetic fields

Fig.3 is a part of SCN shown in Fig.1 that is in the direction of Z-axis. The matched stub (V_{mx}) and short circuit stub (V_{sx}) have been added to SCN node for modeling of magnetic losses and permeability (μ), respectively.

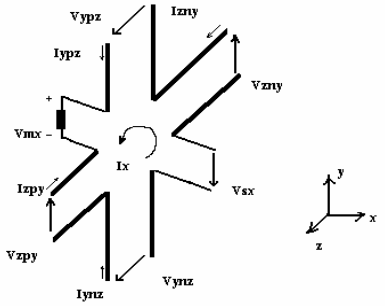

Fig3. GSCN node with short and matched circuit stubs

Basis on Fig.3, we have [6]:

$$I_x = 2\frac{(V^i_{ypz} - V^i_{ynz} + V^i_{zny} - V^i_{zpy} - V^i_{sx})}{Z_{ypz} + Z_{ynz} + Z_{zpy} + Z_{zny} + Z_{sx} + R_{mx}} \quad (5)$$

Using a similar way for I_y and I_z :

$$I_y = 2\frac{(V^i_{xpz} - V^i_{xnz} + V^i_{znx} - V^i_{zpx} - V^i_{sy})}{Z_{xpz} + Z_{xnz} + Z_{znx} + Z_{zpx} + Z_{sy} + R_{my}} \quad (6)$$

$$I_z = 2\frac{(V^i_{xpy} - V^i_{xny} + V^i_{ynx} - V^i_{ypx} - V^i_{sz})}{Z_{xpy} + Z_{xny} + Z_{ynx} + Z_{ypx} + Z_{sz} + R_{mz}} \quad (7)$$

Where, Z_{ipj} and Z_{inj} are the characteristic impedance of transmission lines, Z_{si} is the impedance of short circuit stub and R_{mi} is the resistance of matched stub ($i, j \in x, y, z$).

We can use Equs.5-7 for calculating of magnetic fields in a TLM mesh of $\Delta x \times \Delta y \times \Delta z$ dimension.

$$H_x = I_x / \Delta x, H_y = I_y / \Delta y, H_z = I_z / \Delta z \qquad (8)$$

3- The used equations for structure analysis

For all structures used in this paper, we assume $\mu_r = 1$. These structures have no electrical and magnetic losses, then, we don't add short circuits and matched stubs to SCN node, that is:

$$G_{ei} = R_{mi} = Z_{si} = 0 \qquad (9)$$

The open circuit stubs of y_{0i} are determined from Equ.10, [7]:

$$y_{0i} = 2y_0\left(\frac{\varepsilon_{ri}\sqrt{\mu_0\varepsilon_0}}{\Delta t}\frac{\Delta j \Delta k}{\Delta i} - 2\right) \qquad (10)$$

Using of SCN node for analysis of these structures has been caused by above factors.

Fig.4 illustrates a SCN node:

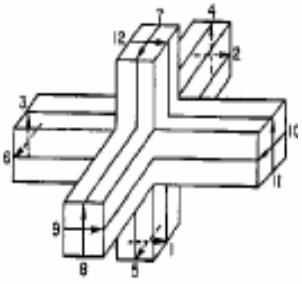

Fig4. A node of SCN-TLM

As it has been shown in Fig.4, the SCN node consists of twelve transmission lines. The characteristic admittance of each transmission line is y_o.

As expressed above and with regards to Fig.4, we can simplify Equs.1-3 as follows:

$$V_x = \frac{2(V_1^i y_0 + V_{12}^i y_0 + y_0 V_2^i + y_0 V_9^i + y_{0x} V_{0x}^i)}{4y_0 + y_{0x}} \qquad (11)$$

$$V_y = \frac{2(V_3^i y_0 + V_{11}^i y_0 + y_0 V_4^i + y_0 V_8^i + y_{0y} V_{0y}^i)}{4y_0 + y_{0y}} \qquad (12)$$

$$V_z = \frac{2(V_6^i y_0 + V_{10}^i y_0 + y_0 V_5^i + y_0 V_7^i + y_{0z} V_{0z}^i)}{4y_0 + y_{0z}} \qquad (13)$$

The Equs.5-7 can be simplified as below:

$$I_x = \frac{2(V_7^i - V_5^i + V_4^i - V_8^i)}{4Z_0} \qquad (14)$$

$$I_y = \frac{2(V_{10}^i - V_6^i + V_2^i - V_9^i)}{4Z_0} \qquad (15)$$

$$I_z = \frac{2(V_{11}^i - V_3^i + V_1^i - V_{12}^i)}{4Z_0} \qquad (16)$$

4- Performing TLM Process and Truncation Error

To perform TLM process, the network is initially excited by voltage impulses. These initial impulses move through network with sequential time steps, and they will be reflected after facing to nodes. The relation between radiated and reflected pulses is determined by S matrix.

We limit the time steps in simulations to save memory and time. This limitation causes a kind of error in conversion process of output response from time domain to frequency domain using Fourier Transform, which is called Truncation error.

The effect of this error is appeared as distortion in output response. This error can be reduced considerably using windowing techniques like Hamming, Square window, Bartlett, Hanning and Welch [8].

The Zero padding method is another technique for Truncation error reduction. In this technique, the Fourier transformation points (n) are increased without increasing of time domain data [9].

5- Choosing Of Mesh Dimensions and Time Step

The effective factors in TLM mesh dimensions are:
1) Maximum operating frequency; it is necessary for stability of a TLM network to choose TLM mesh dimensions smaller than wavelength, then, we must calculate the minimum of wavelengths (λ_{min}) using maximum operating frequency. Therefore:

$$\Delta l << \lambda_{min} \quad (17)$$

2) The dimension of structure; in order to reduce the TLM meshes numbers and save memory and time, we use TLM meshes with greater dimensions when the dimensions of studied structure are very large (ECM room). It means:

$$\Delta l \le 0.1\lambda_{min} \quad (18)$$

3) Non- homogenous meshes; there are some points in some structures like antennas which need more accuracy (near field), for these areas:

$$\Delta l \le 0.01\lambda_{min} \quad (19)$$

In some other points, field calculation needs less accuracy (far field), for these points we choose $\Delta l \le 0.1\lambda_{min}$.

In this paper, we choose maximum operating frequency of $f_{max} = 100GHz$ to analyze structures Therefore $\lambda_{min} = 3000\mu$. With regards to Equs.18-19 and in order to reduce number of nodes, we choose an optimal value for $\Delta l = (1/60)\lambda_{min} = 50\mu$

We calculate time steps in TLM network from positive stub admittance condition. Imposing this condition to Equ.10:

$$\Delta t < \frac{\varepsilon_r \Delta l}{2}\sqrt{\varepsilon_0\mu_0} \Rightarrow \Delta t = \frac{\Delta l}{2c} \quad (20)$$

For investigated structures, we have:

$$\Delta t = \frac{\Delta l}{2c} = \frac{50\mu}{6\times10^8} = 8.33\times10^{-14}\,\text{sec}$$

6- Network Excitation and Characteristic Impedance Calculation

We excite E_z field by imposing voltage impulses to ports 5, 6, 7, 10 of Fig.4 [13]. Exciting of TLM network will inject undesirable modes to the network. To prevent this problem, we should choose bandwidth of exciting pulses as narrow as it is possible. These pulses should be damped in some time steps, therefore, excitation in TLM networks is Gaussian. We use Equ.21 for E_z field calculation in investigated structure:

$$V_5 = V_6 = V_7 = V_{10} = E_{z0}e^{-\frac{(0.1T_t - t)^2}{2\sigma^2}} \quad (21)$$

Where, T_t is total number of time steps, t is the passed time steps and σ is chosen such that the minimum and maximum values of exciting field be satisfied.
Using Equ.13, we can calculate E_y field in each point and each time step. We save it in a vector called TE_y. We can calculate H_z in the same point and time step using Equ.16 and it will be saved in a vector named TH_z. These vectors can be calculated in time domain. We use FFT to transform them to frequency domain (FE_y and FH_z). FE_y and FH_z are E_y and H_z fields in frequency domain. Now, we can calculate characteristic impedance of structures in each frequency using Equ.22:

$$(Z_{oL})_i = \frac{(FE_y)_i}{(FH_z)_i} \quad (22)$$

Where FE_y is the magnitude of E_y field in i^{th} frequency, FH_z is the magnitude of H_z in the i^{th} frequency, and Z_{ol} is the line characteristic impedance in the i^{th} frequency.

7- Numerical Results

We will calculate characteristic impedance of three types of structures using above approach. We consider a $700\mu\times700\mu$ section with the following three structures. These structures will be held in a box of dimensions $40\Delta l\times30\Delta l\times20\Delta l$ and

we excite E_z with $E_{z0}=1\frac{mv}{m}$ and $\sigma=20$ in Equ.21. Total iteration time is $T_t=5000\Delta t$. In Figs.5-7 and Fig.9, You can see the upper view of the structure in left and the front view in right.

7-1 Co-Planner waveguide

Fig.5 illustrates a co-planner waveguide. The specifications of waveguide are:

$$w=5\Delta l, h=5\Delta l, G(gap)=2\Delta l, \varepsilon_r=9.8, \Delta l=50\mu$$

$$L=700\mu, \Delta t=8.33\times10^{-14}\,\text{sec}$$

We excite E_z field by imposing Gaussian pulses as stated before. We calculate H_z and E_y in $(21\Delta l,16\Delta l,8\Delta l)$ and Z_{ol} is determined using Equ.22 in a frequency range of $0<f<100G$. The Z_{ol} is plotted in Fig.6. It can bee seen that characteristic impedance is of value 52Ω in low frequencies and it decreases with increasing frequency. This phenomenon can be explained by assuming the line as a collection of capacitors and inductances. The value of this elements changes when the frequency increases [10].

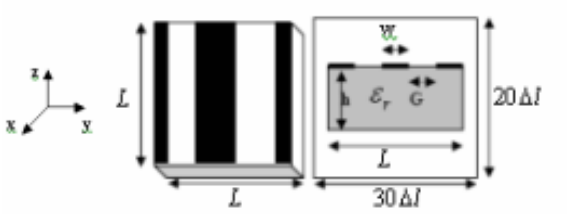

Fig5. The Co-planar waveguide

In this structure, an increase in frequency, will cause a decrease in inductance effects and an increase in capacitance effects, therefore, characteristic impedance will decrease.

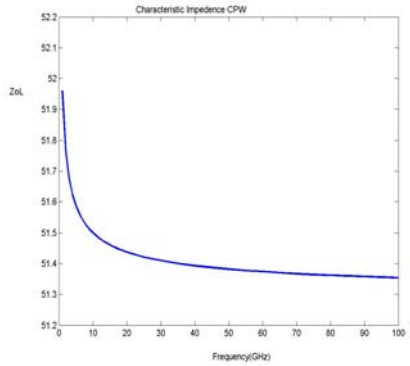

Fig6. The characteristic impedance of CPW versus frequency.

7.2 Grounded co- planner waveguide

Consider the previous structures and dimensions, and also assume that there is a ground in $z=5\Delta l$ as a boundary condition. Fig.8 illustrates characteristic impedance of this structure in $(21\Delta l,16\Delta l,8\Delta l)$. Characteristic impedance is 42Ω for low frequencies. As the same as previous structure and for the same reasons, when the frequency increases, there is a decrease in characteristic impedance. Comparing this two structures show that there is a 10Ω decrease in characteristic impedance if we add e ground plate.

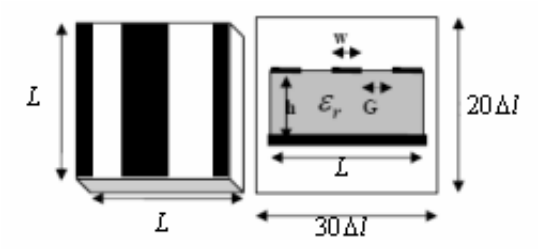

Fig7. The Grounded Co- Planar Waveguide

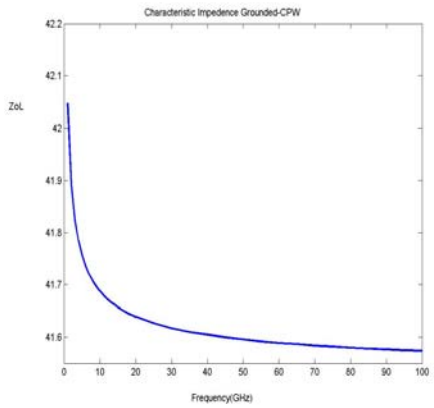

Fig8. The characteristic impedance of GCPW versus frequency.

7.3 Microstrip

Fig.9 shows a microstrip of the following dimensions and specifications:

$$L=700\mu, w/h=1, h=5\Delta l, \Delta l=50\mu, \varepsilon_r=9.8$$

We plot Z_{ol} in frequency domain in Fig.10, when E_z field have been excited like the previous structures.

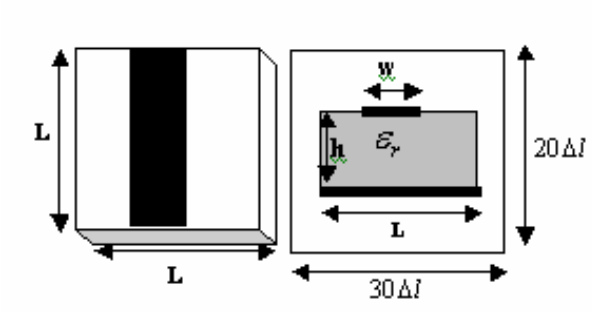

Fig9. The Microstrip

Characteristic impedance of this line in low frequencies is 49.2Ω. Empirical equations introduced in [1, 10] admire this value. In this structure, characteristic impedance increases when frequency increases. Z_{0l} have been computed using Equ.23 (empirical equation) $Z_{oL} = 49.4894\Omega$.

$$Z_{oL} = \frac{377}{2\pi\sqrt{0.5(\varepsilon_r + 1)}}[Ln(\frac{8h}{w}) + (1/32)(\frac{w}{h})^2 - 0.5\frac{(\varepsilon_r - 1)}{(\varepsilon_r + 1)}Ln(\pi/2) + (1/\varepsilon_r)Ln(4/\pi)] \quad (23)$$

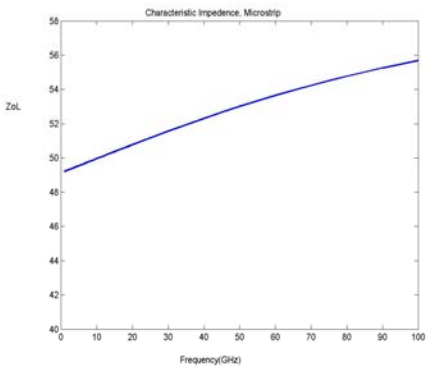

Fig10. The characteristic impedance of Microstrip versus frequency.

8. Conclusion

There is no analytical approach for computing characteristic impedance of structures but there are empirical and experimental relations where can be used for analysis of these structures. We can use these relations up to frequency of 30GHz with some modifications. However, we can not use these relations for high frequencies. In this paper, we compute characteristic impedance of CPW, GCPW and Microstrip structures in frequency range of $0 < f < 100G$ using full wave numerical TLM approach. Comparison of the results with the relations in low frequencies [10], admires the TLM approach results.

9. References

[1] Edwards T.C., M.B.Steer, "Foundations of Interconnect and Microstrip Design," John WILEY & SONS Press, 2000.

[2] Tatsuo Itoh , "Numerical Techniques for Microwave and Millimeter-Wave passive Structures ," JOHN WILEY & SONS,1989.

[3] Qi Zhang and Wolfgang J.R.Hoefer, "Characteristics of new 3D distributed node TLM mesh with cells of arbitrary aspects ratio," IEEE MTT-s Digest, 1994

[4]M.N. Sadiku, "Numerical Techniques in Electromagnetics," CRC Press, 1992.

[5] P.B. Johns, "symmetrical condensed node for the TLM method," IEEE Trans. Microwave Theory Tech. ,vol.35,pp. 370-377, 1987.

[6] Christos Christopoulos, "The Transmission Line Matrix Method," IEEE Press 1995.

[7] Vladica Trenkic and Christos Christopoulos, "Development of a General Symmetrical Condensed Node for the TLM Method," IEEE MTT Vol.44 NO.12 December, pp. 2129-2135, 1996.

[8] L.Albasha and C.M. Snowden," TLM Time-Domain Modeling and the use of Windowing profiles for Frequency-Domain Transformations applied to Microwave Cavity Resonators", IEE conference publication, No.420, 1996.

[9] A.V. Oppenheim and R.W. Schaser, "Discrete–Time Signal Processing", prentice Hall, pp.556 , 1989.

[10] K.C.Gupta , Ramesh Garg ,I.J.Bahl , " Microstrip Lines and Slotlines, " ARTECH Press 1979.